Design of compact bi-directional triplexer based on silicon nanowire waveguides

Wei Ling (凌 伟), Zhen Sheng (盛 振)*, Chao Qiu (仇 超), Hao Li (李 浩), Aimin Wu (武爱民), Xi Wang (王 曦), Shichang Zou (邹世昌), and Fuwan Gan (甘甫烷)**

State Key Laboratory of Functional Materials for Informatics, Shanghai Institute of Microsystem and Information Technology, Chinese Academy of Sciences, Shanghai 200050, China

**Corresponding author: zsheng@mail.sim.ac.cn;* ***corresponding author: fuwan@mail.sim.ac.cn*

Received December 5, 2012; accepted March 13, 2013; posted online March 20, 2013

A compact bi-directional (BiDi) triplexer using grating-assisted multimode interference (MMI) coupler is proposed based on silicon nanowire waveguides.Because of the high index contrast between silicon and silicon dioxide, the size of the structure is greatly reduced with a footprint of 2.5×911 (μm). Asymmetrical ports are introduced in the MMI structure to satisfy the bandwidth requirements of the industrial standards ITU-T G.983.3-dB bandwidths of 100, 22, and 15 nm are obtained for the wavelengths of 1 310, 1 490, and 1 550 nm, respectively. The device can be readily fabricated using a commercial CMOS process.

OCIS codes: 130.3120, 230.7390, 060.4230.
doi: 10.3788/COL201311.041301.

Fiber-to-the-home (FTTH) system has been developed to meet the ever-increasing demand for bandwidth. Bi-directional (BiDi) triplexer, as one of the key components in FTTH system,is widely used to provide a triple play service, i.e., the wavelengths of 1 310, 1 490, and 1 550 nm carry upstream data, downstream data, and downstream video signals, respectively. Thin film filters based triplexers are commonly used today to de/multiplex these signals[1]. However, it is difficult to integrate and package them with other devices,making them bulky and costly. Photonic integration scheme based on planar lightwave circuits (PLCs) is a promising solution to reduce the size of triplexers and is also suitable for volume production at low cost[2]. Several designs based on PLCs have been reported[3−6]. Although the devices proposed in Refs. [3, 4] can successfully de/multiplex three up-and down-stream channels, it is difficult for these structures to meet the bandwidth requirements of the industrial standards ITU-T G.983, where 3-dB bandwidths of 100, 20, and 10 nm for wavelengths λ =1 310, 1 490, and 1 550 nm are required respectively[7]. Novel structures were proposed[5,6] to fulfill the bandwidth requirements. However, the sizes of these devices are still quite large (typically 36×7 000 (μm)) since they are based on silica waveguides with a low index contrast. Another solution for compact triplexer is based on photonic crystals[8], which may have even more compact sizes, but their bandwidths are limited.

In recent years, silicon based photonic devices are becoming more and more attractive for practical application.The high refractive index contrast between silicon and SiO_2 offers a strong light confinement, making it possible to construct waveguides with sub-micron cross-sections and bending radii less than 5 μm. The process compatibility with commercial CMOS technology would also reduce the fabrication cost greatly.Low loss silicon nanowire waveguides and various devices have been demonstrated[9,10], indicating their great potential for practical applications.Recently, a compact triplexer based on sub-micron silicon rib waveguide was demonstrated[11]. While the total length of the device-was only 400μm, it fails to meet the bandwidth requirements.

In this letter, a compact BiDi triplexer is designed based on silicon nanowire waveguides. Grating-assisted multi-mode interference (MMI) coupler is employed in the device and the BiDi beam propagation method (BiBPM) is used to optimize the structure. To satisfy the bandwidth requirements for different channels, asymmetric tapered ports are introduced.The footprint of the optimal device is only 2.5×911 (μm).

The schematic of the triplexer is illustrated in Fig. 1. It consists of a 2×2 MMI coupler with a shallow-etched Bragg-grating defined in the multimode waveguide region.Downstream data and downstream video signals at 1 490 and 1 550 nm wavelengths are downloaded from port 1 to port 2 and port 4, respectively, while upstream data carried by 1 310 nm wavelength is uploaded from port 3 to port 1. Considering the bandwidth specifications required by the standard, especially the large bandwidth for the wavelength of 1 310 nm, the Bragg-grating is used to reflect the signal at 1 310 nm wavelength from port 3 to Port 1. Both the etching depth and the number of period are carefully designed to meet the demands on the bandwidth and the extinction ratio. For the down-stream signals at 1 490 and 1 550 nm wavelengths, the MMI coupler functions as a coarse wavelength-division multiplexing (WDM) to de/multiplex them from port 1 to

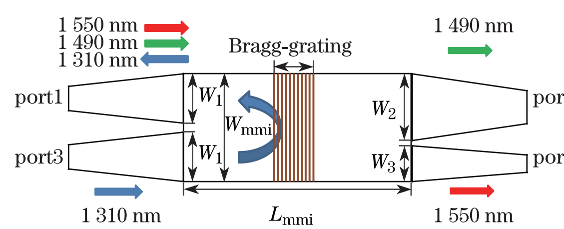

Fig. 1. Schematic configuration of the present triplexer.

port 2 and port 4, respectively. Tapered ports are used to reduce the loss and ensure an adiabatic transition. The device is based on silicion-on-insulator (SOI) wafers with top silicon of 220 nm and buried oxide (BOX) of 2 μm.

Bragg-grating is designed in this structure to upload the signals at 1 310 nm wavelength from port 3 to port 1. Shallow-etched slots are defined in the multimode waveguide region to form the Bragg-gratings.The grating period Λ is determined by

$$\Lambda = m\lambda_0/2n_{\mathrm{eff}}, \tag{1}$$

where n_{eff} is the effective refractive index of the grating region, λ_0 is the central wavelength of reflection and m is the diffraction order. BiBPM[12] is used to design the Bragg-grating. TE mode is assumed in the simulation. To satisfy the large bandwidth requirement for 1310 nm and achieve a high reflection, both the etching depth and the grating number of the Bragg-grating are optimized.

The influence of the etching depth and the period number on the reflection and bandwidth are first simulated and shown in Fig. 2. One sees that as the etching depth increases, both the reflection and bandwidth increase accordingly, while the increase of the period number of grating leads to an increase of reflection and a decrease of the 3-dB bandwidth. Considering the bandwidth and extinction ratio specifications for the 1 310 nm wavelength, an etching depth of 70 nm and a period number of 30 are chosen, while the Bragg-grating period Λ is set to be 232 nm to reflect the wavelength of 1 310 nm according to Eq. (1). This design gives a reflection of 98.7% and a 3-dB bandwidth of 100 nm at 1 310 nm, as shown in Fig. 3. On the contrary, the grating structure poses little influence on the down-stream signals as the reflections at 1 490 and 1 550 nm are only 0.76% and 0.32%, respectively. Besides, the excess loss and extinction ratio are calculated to be –0.51 and –20.7 dB, respectively.

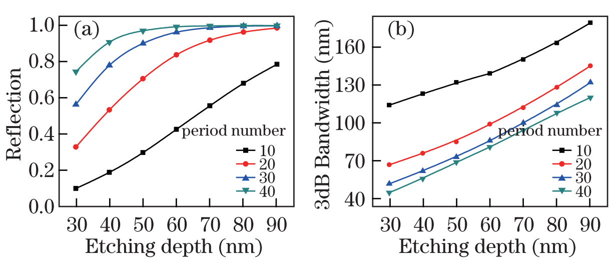

Fig. 2. (a) Reflection and (b) 3-dB bandwidth for different etching depths and grating period number.

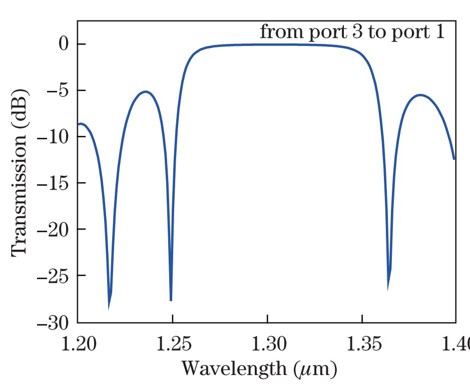

Fig. 3. Spectral responses at 1 310-nm wavelength.

In order to achieve the function of triplexer, we need to embed the Bragg-grating into the MMI coupler. Here, the MMI coupler functions as a coarse WDM to de/multiplex the down-stream signals at λ=1 490 and 1 550 nm. The operation principle of the MMI coupler is based on the self-imaging effect[13]: a number of modes are stimulated in the multimode region and the input field is reproduced in single or multiple images at periodic intervals along the multimode waveguide. Define L_π as the beat length of the two lowest modes, which can be expressed as

$$L_\pi = 4n_{\mathrm{c}}W_{\mathrm{e}}^2/\lambda_0, \tag{2}$$

where n_{c} and W_{e} represent the effective refractive index and the effective width of the multimode section,respectively,and λ_0 is the wavelength in free space.As the imaging position is related to L_π, which is dependent on λ_0, as shown in Eq. (2), different wavelengths can be separated as they have different imaging positions. The direct and mirrored images can be produced at $L = p(3L_\pi)$, p=0, 1, 2, $\cdots$, for p even and p odd, respectively. Therefore, when the length of the multimode waveguide is set to be an even multiple and an odd multiple of the beat lengths for 1 490 and 1 550 nm, respectively, the two wavelengths can be separated and output via the through-path and cross-path, respectively. In our design, the width of MMI coupler (W_{mmi}) is set to be 2.5 μm, and the optimized grating is shallow-etched in the multimode region. To meet the single mode condition, 0.5×0.22 (μm) is chosen as the size of the input/output waveguides. Linear tapers are used to broaden the input/output waveguides to reduce the mode mismatching loss between them and the multimode region[14]. All of the four ports are set to be 1.2 μm wide initially. Figure 4 shows the propagation powers of 1 490 and 1 550 nm for different paths.One sees that the power alternates between the through-path and the cross-path for each wavelength. Since the field distributions for the two wavelengths are different along the propagation direction, an optimal MMI length (L_{mmi}) can be found so that the power for one of the wavelengths is output to the through-path while that for the other wavelength is output to the cross-path. Therefore, the two wavelengths are demultiplexed.

From the simulation result shown in Fig. 4, we can see that the signal at 1 490 nm wavelength reproduces itself in the through-path while that at 1 550 nm wavelength is imaged in the cross-path for L_{mmi}= 851.5 μm. The propagation field distributions for the two wavelengths are shown in Fig. 5. One sees that the two wavelengths are separated successfully to each output port.We also calculate the excess loss and the extinction ratios for the two ports, the excess loss are –0.42 and –0.52 dB while the extinction ratios are –19.6 and –21dB for 14 90 and 1 550 nm, respectively.However, 3-dB bandwidths of 17 and 18 nm are obtained for 1 490 and 1 550 nm wavelength, respectively, which fail to meet the bandwidth requirement of 20 nm at 1 490 nm according to ITU-T G.983. To solve this problem, asymmetric tapered ports are introduced in the MMI structure. A wider port(port 2) is used for the 1 490 nm channel which allows a larger range of wavelengths to couple into the output port, thus broadening the bandwidth. After optimization, the width for port 2

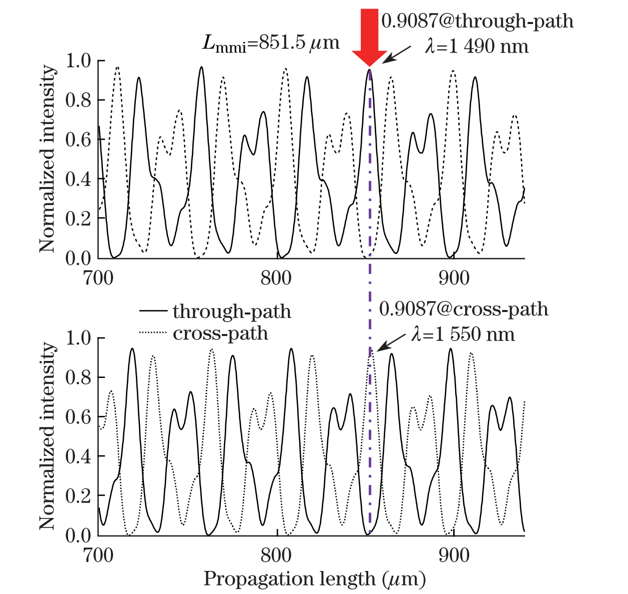

Fig. 4. Transmission power both in through-path and cross-path for the wavelengths of 1 490 and 1 550 nm.

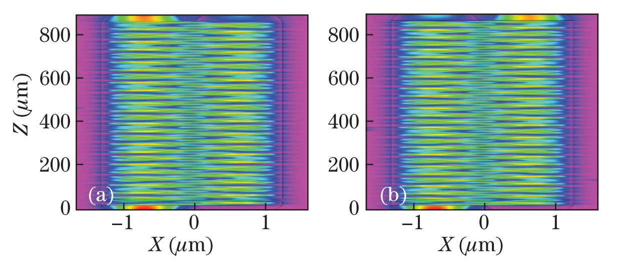

Fig. 5. Propagation electric field distributions of the triplexer for the two wavelengths of (a) 1 490 and (b) 1 550 nm.

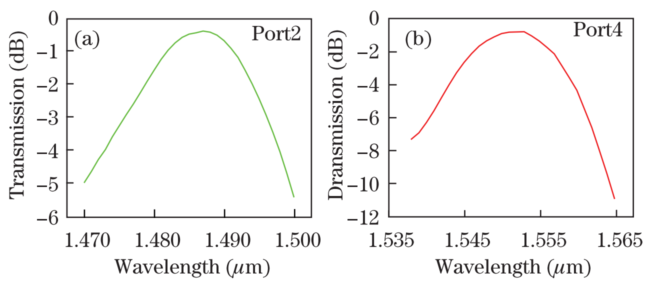

Fig. 6. Spectral responses at (a) 1 490- and (b) 1 550-nm wavelength.

Table 1. Performance Parameters of the Optimal Triplexer

Wavelength Channel (nm)	Parameter		
	3 dB Bandwidth (nm)	Excess Loss (dB)	Extinction Ratio (dB)
1 310	100	–0.51	–20.7
1 490	22	–0.65	–26.3
1 550	15	–0.81	–20.2

(W_2) is chosen as 1.4 μm while the width for port4 (W_3) is chosen as 0.9 μm. The resulting spectral responses at port2 and port4 are shown in Fig. 6. It shows that the bandwidth for 1 490 nm increases to 22 nm, while that for 1 550 nm is 15 nm, satisfying the bandwidth requirement. Because of the asymmetric tapered output ports, there is mode mismatching between the imaging field and the two output ports, which slightly increases the excess loss of the triplexer. Finally, the performance parameters of the optimal design are summarized in Table 1. The excess loss and the extinction ratio are less than 1 dB and lower than –20 dB, respectively, for all of the three wavelength channels, while the bandwidth specifications fulfill the ITU-T G.983 standard.

In conclusion, a compact BiDi triplexer is proposed based on silicon nanowire waveguides. Grating-assisted MMI coupler is employed in the device. Because of the high index contrast between silicon and silicon dioxide, the size of the structure is greatly reduced with a footprint of 2.5×911 (μm). To satisfy the bandwidth requirements in ITU-T G.983, asymmetrical ports are introduced in the MMI structure and 3-dB bandwidths of 100, 22, and 15 nm are obtained for 1 310, 1 490, and 1 550 nm, respectively. The optimal device also has a good performance in terms of low excess loss and large extinction ratio. Besides, the device can be readily fabricated using a commercial CMOS process, making it quite low cost.

This work was supported by the Science and Technology Commission of Shanghai Municipality (Nos. 10DJ1400400 and 10706200500), the National "863" Project of China (No. 2012AA012202), the Natural Science Foundation of Shanghai (No. 11ZR1443700), and the National Natural Science Foundation of China (Nos. 61106051, 61107031, and 61275112).

References

1. J. H. Song, J. H. Song, K.-Y. Kim, J. Cho, D. Han, J. Lee, Y. S. Lee, S. Jung,Y. Oh, D.-H. Jang, and K. S. Lee, IEEE Photon. Technol. Lett. **17,** 1668 (2005).
2. M. Fuller, Lightwave **21,** 24 (2004).
3. J. Li, J. An, Y. Wu, J. Li, H. Wang, and X. Hu, Chin. Opt. Lett. **8,** 060588 (2010).
4. X. Lin, T. Lang, and J. He, J. Lightwave Technol. **29,** 1407 (2011).
5. C. L. Xu, X. Hong, and W. Huang, Opt. Express **14,** 4675 (2006).
6. J. Song and J. F. Ding, Electron. Lett. **46,** 1213 (2010).
7. ITU-T G.983.3, "A broadband optical access system with increased service capability by wavelength allocation".
8. H. Ren, J. Ma, W. Wen, Y. Qin, Z. Wu, W. Hu, C. Jiang, and Y. Jin, Chin. Opt. Lett. **9,** 042501 (2011).
9. W. Bogaerts, S. K. Selvaraja, P. Dumon, J.Brouckaert, K. De Vos, D. Van Thourhout, and R. Baets, J. Sel. Top. Quantum Electron. **16,** 33 (2010).
10. Z. Zhou, Z. Tu, B. Yin, W. Tan, L. Yu, H. Yi, and X. Wang, Chin. Opt. Lett. **11,** 012501 (2013).
11. Y. Shi, S. Anand, and S. He, J. Lightwave Technol. **27,** 1443 (2009).
12. H. Rao, R. Scarmozzino, and R. M. Osgood, Jr., IEEE Photon. Technol. Lett. **11,** 830 (1999).
13. J. Zhou, H. Shen, R. Jia, H. Liu, Y. Tang, C. Yang, C. Xue, and X. Liu, Chin. Opt. Lett. **9,** 082303 (2011).
14. Y. Shi, D. Dai, and S. He, Opt. Commun. **253,** 276 (2005).